Impact toughness of closed cell aluminum foam

Sourav Das*

Mechanical Engineering Department, University of Wisconsin Milwaukee College of Engineering & Applied Science 53211

*Corresponding author

DOI: 10.5185/amp.2018/1432
www.vbripress.com/amp

Abstract

The impact toughness of closed-cell aluminum foam with various densities was investigated using Charpy impact. The impact load history revealed an elastic region followed by a rapid load drop region. The peak load and impact toughness of aluminum foam increase exponentially with density. The power exponents for the impact toughness test are greater than that of the compressive test. Fracture analysis indicated a mixed-rupture mode of quasi-cleavage and small shallow dimples. It can be attributed to the complex state of stress of notched specimens and elevated impact velocity under impact loading. Copyright © 2018 VBRI Press.

Keywords: Metal foam, charpy test, impact toughness, energy absorption.

Introduction

In the last several years, the application of metal foam to the energy absorbing and damping field has been paid increasing attention. Therefore, many studies on the quasi-static and dynamic Compressive properties of open-cell **[1–5]** and closed-cell **[6–12]** aluminum foams, thus, have been reported. The results focused on compressive stress-strain behavior, features of energy dissipation and deformation mechanisms of aluminum foam, offer a useful reference for designing the cushioning devices and shock absorber. However, closed-cell aluminum foam made by melt route and powder route often contains a considerable number of defects, such as microcracks and micropores **[13-16]**, which would influence the failure and fracture processes. To date, few studies focus on the toughness of metal foam, which is important for estimating the service performance of materials under transient dynamic load conditions. The mechanical response of specimen with crack is quite different from that of one without a crack. It is, thus, necessary to conduct a proper assessment of the dynamic fracture behavior of closed-cell aluminum foam for structural application. One method is to investigate the impact toughness of the notched specimen by means of the Charpy impact test. However, the only data one could obtain by this test is impact toughness value (*Ak*), which can't reflect the load history during loading. The Drop hammer (Instron9250HV) including a drop tower testing machine, instantaneous force and distance measurement system and a data acquirement system, is an appropriate tool in practical applications for characterizing and evaluation of force and energy of aluminum foam under impact loading. It needs to be emphasized that the test can't be used for quantitative toughness evaluation or safety predictions.

Experimental

Aluminum (purity 99.7%) was used as the materials for foaming. High purity Ca (3 *wt*.%) was introduced into molten aluminum, to enhance the viscosity of the Al melt. TiH_2 powder (size: 40-50μm, 1.5 *wt*.%) was used as the foaming agent. Further processing details of foam making are available in Ref. **[17]**. However, in the present study, the surface of the molten aluminum was covered by an asbestos gland and iron with certain mass during the foaming process. The goal here is to improve essentially the heat-preservation property of the surface of melt as well as extra foaming pressure. In this way, aluminum foams with smaller and more homogeneous pore size were successfully fabricated. The apparent densities (ρ) of the foams were measured and found in the range of 0.30-0.75 g/cm^3. The cell size of these foams was measured and found approximately in the range of 0.5-2.5mm.

Impact tests were performed with standard size specimens with a dimension of 55×10×10 mm^3 equipped with 45° V-shaped notch of 2 mm depth and 0.25 mm root radius at the tip of the notch. The specimen was supported by anvils of 40 mm support span. The specimen was impacted at a velocity of 1.5 m/s. The total energy provided by the striking hammer, in this study, reached up to 50J, which is much larger than the energy absorbed (less than 1J) by notched foam specimens. High energy tests are favorable for foam specimens, as a loss in energy of striker becomes negligible during the impact process, and accordingly, the loading rate stays practically constant over the entire failure process **[18]**. The impact energy, dissipated by foam specimen, is then calculated by integration over the entire load-displacement curve. The impact toughness, *Ak* (J/cm^2),

is taken to be the impact energy divided by the area (0.8cm×1cm)

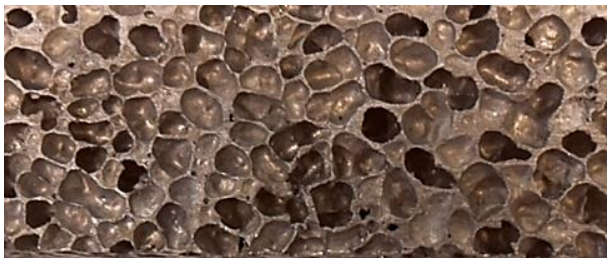

Fig. 1. Closed cell Aluminum foam.

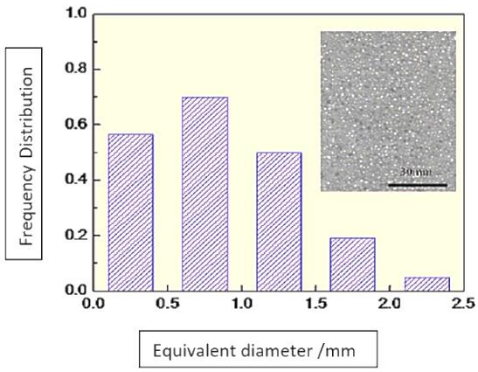

Fig. 2. Distribution of cell size and macro-morphology (insets) of closed-cell aluminum foam with a density of 0.48g/cm^3.

Results and discussion

Typical cell size distribution and macro-morphology of foam specimens tested are showed in **Fig. 1**. It was found that the cells with a diameter less than 1.5mm account for more than 85%. The evenly distributed porosity (insets in **Fig. 2**) was observed for all test specimens. These features of foam specimens cannot only ensure the repeatability and consistency of the test results but also avoid the side effect due to fewer cells in the loading direction.

Fig. 3 shows a typical set of data obtained for the foam specimens with average density (ρ) of 0.40g/cm^3, 0.51g/cm^3, and 0.69g/cm^3 tested at an impact velocity of 1.5m/s. Four measurements for specimens with similar density were conducted to evaluate the impact toughness.

Fig. 3 (a)-(c) represent the impact force history, in which an elastic region in the early stage followed by a rapid drop region once the force exceeds a peak. The specimens with similar density exhibit almost constant peak load. Also, the impact velocity curves as shown in **Fig. 3 (a)-(c)** maintains at about 1.5m/s. It indicates a good stability and repeatability of impact response for foam specimens. The area under the load-displacement curve represents the absorbed energy. Peak load and impact energy increase with increasing density. Additionally, **Fig. 3 (d)** is the compressive stress-strain curves and energy absorption (strain energy density) curves for specimens with average density of 0.40g/cm^3, 0.51g/cm^3 and 0.69g/cm^3. The strain energy density here is taken to be the energy at the strain of 0.5 (*E0.5*).

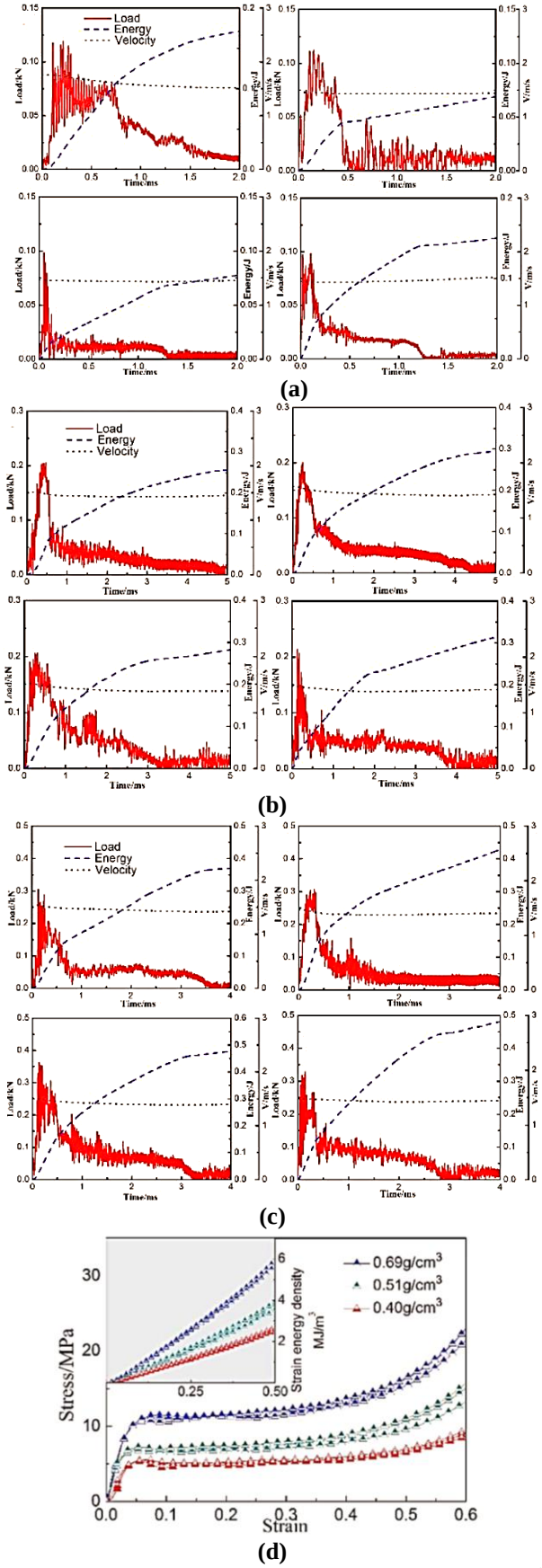

Fig. 3. Charpy notched impact load and energy vs. time curves of aluminum foam with density of (a) 0.40g/cm^3; (b) 0.51g/cm^3; (c) 0.69g/cm^3 and (d) corresponding compressive stress-strain curves and energy absorption curves.

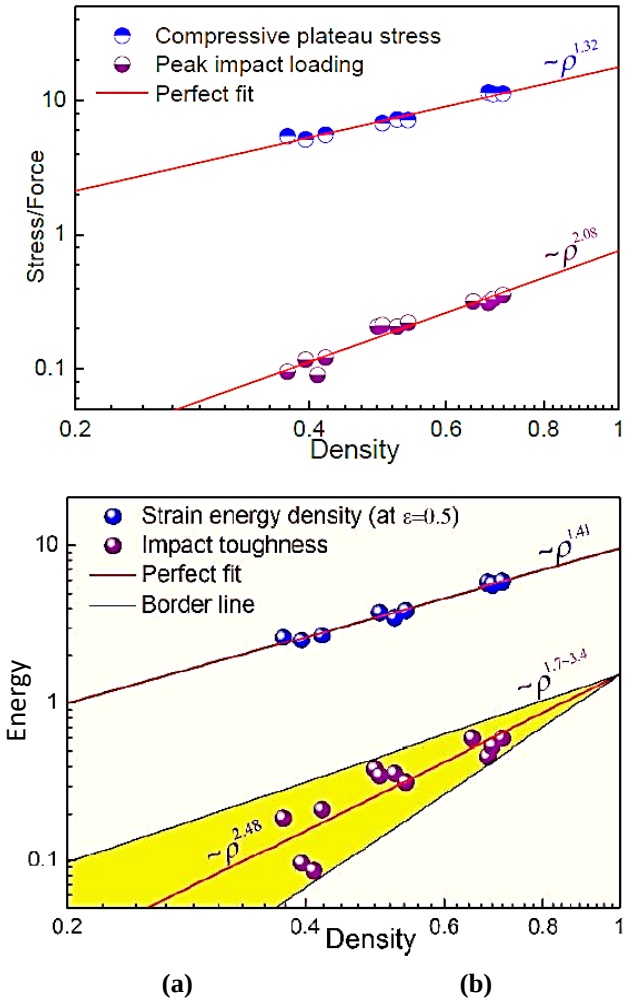

Fig. 4. Compressive plateau stress/peak impact load of closed-cell aluminum foams vs. density (a) and strain energy density/impact toughness vs. density (b).

The relationships between density and impact loading are shown in **Fig. 4 (a)**. The density dependence of compressive plateau stress (σ_p) was also shown in **Fig. 4 (a)** for comparison. The fitting results revealed a power function relation between peak impact loading/compressive plateau stress and density. The power exponent for impact is 2.08, and for compression, 1.32. It seems that impact loading is more sensitive to density than compressive stress for closed-cell aluminum foam. It may be related to the impact strengthening of foam structure **[19]** and the strain rate effect of cell wall materials **[11]**.

Fig. 4 (b) shows the strain energy density and impact toughness, *Ak*, of closed-cell aluminum foams as a function of density. It is evident from this figure that the energy absorption of foam by compression and impact also follows a power law relationship with density. The power exponent for impact is 2.48, more than twice that for compression (1.41). According to Gibson and Ashby model **[20]**, both the plateau stress and strain energy density of open cell foam follows power function relation with density with an identical exponent of 1.5. In the present work, the closed-cell aluminum foam shows a higher exponent (2.0-2.5) for peak impact load and impact toughness.

Elevated impact velocity is probably the principal contributor to high-density sensors.

The fracture surfaces of compressive specimen and impact specimen were observed to reveal the micro-deformation features. **Fig. 5 (a)** shows typical ductile fracture with many slip lines and deep dimples for compressive fracture, indicating that plastic deformation took place in the α-Al solid solution resulting in the formation of the dimples bands. The impact of fracture morphology is shown in **Fig. 5 (b)**. Although there were some ductile fracture features in impact fracture surface just like a compressive fracture, a considerable amount of fracture surface shows a mixed-rupture characteristic of quasi-cleavage and small shallow dimples. The secondary cracks generated from brittle Al (Ca, Ti) phase **[21]** can be observed in **Fig. 5 (b)**. The complex state of stress of notched foam specimens and elevated impact velocity is responsible for the distinguishing fracture mode.

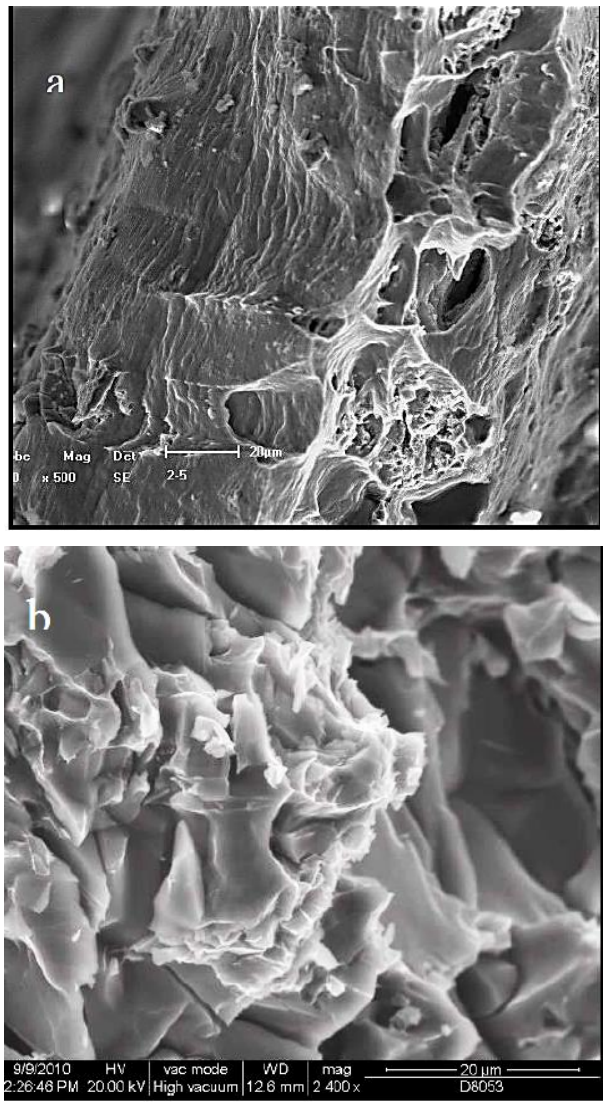

Fig. 5. Typical fracture surface morphology for (a) compressive test and (b) impact toughness test.

Conclusions

The closed-cell aluminum foams with cell size range from 0.5-2.5mm were successfully fabricated. The impact load/energy-time curves were used to characterize the impact fracture process of aluminum foam. Repeatable and stable data were obtained to investigate the impact toughness of foam specimens. The compressive stress-strain response was also investigated for comparison. Both compressive plateau stress/impact peak load and energy absorption/impact toughness exponentially increased with density of foam specimens. The power exponents for the impact toughness test were greater than that for the compressive test. Fracture analysis indicated a mixed-rupture mode of quasi-cleavage and small shallow dimples for impact fracture. The complex state of stress of notched foam specimens and elevated impact velocity was responsible for the distinguishing fracture mode between compression and impact toughness.

References

1. E. Amsterdam, J.H.B. de Vries, J.Th.M. De Hosson, P.R. Onck, The influence of strain-induced damage on the mechanical response of open-cell aluminum foam. *Acta Mater;* **2008**, *56*, 609.
2. E. Amsterdam, J.Th.M. De Hosson, P.R. Onck, on the plastic collapse stress of. open-cell aluminum foam. Scripta Mater.; **2008**, *59*, 653.
3. Wen-Yea Jang, Stelios Kyriakides, on the crushing of aluminum open-cell foams: Part I. Experiments. Int. J. Solids Struct.; **2009**, *46*, 617.
4. Wen-Yea Jang, Stelios Kyriakides, On the crushing of aluminum open-cell foams: Part II analysis. Int. J. Solids Struct.; **2009**, *46*, 635.
5. P.J. Tan, S.R. Reid, J.J. Harrigan, On the dynamic mechanical properties of open cell metal foams-A re-assessment of the 'simple-shock theory'. Int. J. Solids Struct.; **2012**, *49*, 2744.
6. R.P. Merrett, G.S. Langdon, M.D. Theobald, The blast and impact loading of aluminum foam. Mater. Design; **2013,** *44*, 311.
7. G. Castro, S.R. Nutt a, X. Wenchen, Compression and low-velocity impact behavior of aluminum syntactic foam. *Mater. Sci. Eng. A;* **2013**, 578, 222.
8. M. Saadatfar, M. Mukherjee, M. Madadi, G.E. Schro der-Turk, F. Garcia-Moreno, F.M. Schaller, S. Hutzler, A.P. Sheppard, J. Banhart, u. Ramamurthy. Structure and deformation correlation of closed cell aluminum foam subject to uniaxial compression. *Acta Mater.;* **2012**, *60*, 3604.
9. M. Mukherjee, U. Ramamurty, F. Garcia-Moreno, J. Banhart, Solidification of metal foams. *Acta Mater.;* **2010**, 58, 5031.
10. X.F. Tao, Y.Y. Zhao, Compressive failure of Al alloy matrix syntactic foams manufactured by melt infiltration; *Mater. Sci. Eng. A;* **2012**, *549*, 228.
11. Y.L. Mu, G.C. Yao, Z.C. Cao, H.J. Luo, G.Y. Zu, Strain-rate effects on the compressive response of closed-cell copper-coated carbon fiber/aluminum composite foam; Scripta Mater.; **2011**, *64*, 61.
12. Y.L. Mu, G.C. Yao, L.S. Liang, H.J. Luo, G.Y. Zu, Deformation mechanisms of closed-cell aluminum foam in compression; *Scripta Mater.;* **2010**, *63*, 629.
13. M. Mukherjee, F. Garcia-Moreno, J. Banhart, Defect generation during solidification of aluminum foams; *Scripta Mater;* **2010,** *63*, 235.
14. M. Mukherjee, U. Ramamurty, F. Garcia-Moreno, J. Banhart, The effect of cooling rate on the structure and properties of closed-cell aluminum foams. *Acta Mater.;* **2010**, *58*, 5031.
15. Y.L. Mu, G.Y. Zu, Z.K. Cao, G.C. Yao, Q.D. Wang, Metal foam stabilization by copper-coated carbon fibers.; *Scripta Mater;* **2013**, 68, 459.
16. H.J. Yu, G.C. Yao, X.L. Wang, Y.H. Liu, H.B. Li, Sound insulation property of Al-Si closed-cell aluminum foam sandwich panels. *App. Acoust.;* **2007**, *68*, 1502.
17 T. Miyoshi, M. Itoh, G. S. Akiyama, A. Kitahara, Aluminum Foam, "ALPORAS": The Production Process, Properties, and Applications, J. Banhart, M.F. Ashby, N.A. Fleck (Eds): Metal Foams and Porous Metal Structures. © ttiT Verlag (1999)125.
18. J.F. Kalthoff, Characterization of the dynamic failure behavior of a glass fiber/ vinyl-ester at different temperatures by means of instrumented Charpy impact testing. *Compos. Part B;* **2004,** *35*, 657.
19. P.J. Tan, S.R. Reid, J.J. Harrigan, Z. Zou, S. Li, Dynamic compressive strength properties of aluminum foams. Part II-'shock' theory and comparison with experimental data and numerical models. J Mech. Phys. Solids; **2005**, *53*, 2174.
20. L.J. Gibson, M.F. Ashby, Cellular Solids: Structure and Properties, Cambridge University Press, **1997**.
21. H.J. Yu, G.C. Yao Y.H. Liu, the Tensile property of Al-Si closed-cell aluminum foam. Trans. *Nonferrous Met. Soc. China*, **2006,** *16*, 1335.

